

Primary Structural Transformations of Water-Soluble Polysaccharides in the Granulated Juice Sacs of *Citrus changshanensis*

Xuemin Zhang, Xuanang Zheng, Haojie Wang, Chen Kang, Rong Jin, Dengliang Wang, Shaojia Li, Yue Wang, Bo Zhang, Jinping Cao,* and Chongde Sun



Cite This: <https://doi.org/10.1021/acs.jafc.5c05802>



Read Online

ACCESS |

Metrics & More

Article Recommendations

Supporting Information

ABSTRACT: Granulation is a commonly seen internal disorder of citrus fruit, characterized by decreased juice yield, thickened cell wall, and abnormal hardened juice sac. The present study compared the juice sacs of *Citrus changshanensis* at different granulation degrees (healthy, gelatinous, moderately granulated, and severely granulated) regarding their soluble polysaccharide content and structural changes of water-soluble polysaccharides. The contents of water-, CDTA-, Na₂CO₃⁻, 1 mol/L KOH-, and 4 mol/L KOH-soluble polysaccharides increased with the granulation degree. The water-soluble polysaccharides were further fractionated into water eluent (WA), 0.05 mol/L NaCl eluent (0.5S), 0.1 mol/L NaCl eluent (1S), and 0.2 mol/L NaCl eluent (2S) by DEAE-Sepharose chromatography. The detailed structure of these fractions was analyzed using high-performance liquid chromatography, Fourier transform infrared spectroscopy (FT-IR), and nuclear magnetic resonance spectroscopy. Structural changes were evident in the granulated samples compared to the healthy samples, especially in the 0.5S and 1S fractions. As granulation progressed, the degree of methyl esterification in homogalacturonan (HG) regions decreased, and the proportion of rhamnogalacturonan I (RG-I) regions increased. Concurrently, the branching side chains of RG-I, composed of arabinans and arabinogalactans, increased significantly. In line with these structural changes, the viscosity of the water-soluble polysaccharide fractions also increased with granulation degree.

KEYWORDS: citrus, juice sac, granulation, cell wall, polysaccharides

1. INTRODUCTION

Juice sac granulation is a prevalent internal disorder in citrus fruit that occurs during fruit development or during the postharvest period. It is typically triggered by inappropriate environmental conditions, inherent physiological characteristics, or the natural senescence of the fruit.^{1–3} Granulated citrus fruit exhibits significantly reduced commercial value due to the abnormal hardening and juicelessness of the granulated juice sacs. These changes result in poor textural properties and a lack of flavor, making them less appealing for consumption.^{4,5} Thus, juice sac granulation might cause a huge loss to the citrus industry.

The progression of citrus juice sac granulation is a prolonged and dynamic process. For the purpose of facilitating physiological research, the granulation process of juice sacs is artificially categorized into three to four distinct stages based on the morphological characteristics of the tissue.^{6,7} In the initial stage of granulation, the juice sacs become enlarged and begin to exhibit a gelatinous interior. As granulation advances, the juice sacs lose their transparency, becoming hard and opaque white. Ultimately, the juice sacs turn deep cloudy white or yellow and may even exhibit signs of shrinkage in appearance.

Cell wall thickening is a prominent physiological characteristic of granulated citrus juice sacs, primarily due to the increasing accumulation of cell wall components, including pectins, cellulose, and lignin.^{7–10} Lignin accumulation has been identified as a significant physiological change during

granulation and has been extensively studied in pomelo fruit.^{9,11,12} However, in certain citrus species, such as Huyou (*Citrus changshanensis*) and Harumi tangor, the increased accumulation of cell wall polysaccharides, including water-soluble pectin (WSP), sodium carbonate-soluble pectin (SSP), chelate-soluble pectin (CSP), and cellulose, has been determined to be the primary event in the early stages of juice sac granulation, rather than lignin accumulation.^{7,13} Therefore, elucidating the dynamic changes in cell wall polysaccharides is essential to understanding the early biological events occurring during granulation. Studies have shown that the total contents of pectins (including WSP and CSP), hemicellulose, and cellulose increase when calculated based on tissue weight during granulation.^{7,14} However, the extent of accumulation may vary among the different components. This variation can lead to changes in the composition of the cell wall. For example, in the granulated vesicles of grapefruit, the proportion of WSP, CSP, and hemicellulose in ethanol-insoluble solids decreases, whereas the proportion of cellulose increases slightly.^{7,14} Conversely, in

Received: May 10, 2025

Revised: July 4, 2025

Accepted: July 25, 2025

the collapsed vesicles of grapefruit, the proportion of WSP, hemicellulose, and cellulose decreases, while the proportion of CSP increases in ethanol-insoluble solids.⁸ Thus, differentiated accumulation of different polysaccharide components in the cell wall might also be important for the development of granulation.

Beyond alterations in the content of cell wall polysaccharides, structural modifications may also take place during the granulation process. However, while changes in content have been extensively documented, the structural alterations of cell wall polysaccharides in granulated juice sacs remain relatively underexplored. To date, most structural analyses have centered on pectins and hemicelluloses, largely due to their water-soluble nature. For example, atomic force microscopy (AFM) has unveiled that WSP in granulated pomelo juice sacs shows increased chain length and width.¹⁴ In contrast, gel filtration chromatography (GPC) results indicate that the molecular weight of WSP and hemicellulose in the granulated vesicles of grapefruit remains largely stable.⁸ Moreover, in collapsed vesicles, the proportion of small-molecular-weight pectins and hemicellulose rises, while that of large-molecular-weight pectins and hemicellulose declines.⁸

Investigations into the primary structure of cell wall polysaccharides have revealed that the proportion of most neutral monosaccharide components tends to rise in both granulated and collapsed vesicles.⁸ The degree of esterification decreases in water-soluble and EDTA-soluble polysaccharides from granulated juice sacs, whereas the degree of acetylation remains relatively stable with only minor fluctuations.¹⁵ However, an increase in the methyl esterification level of insoluble pectin has been noted in the granulated juice sacs of sweet oranges.¹⁶ Given these varied findings, it is essential to employ a multifaceted technical strategy to thoroughly analyze and interpret the structural transformations of cell wall polysaccharides within a unified research framework.

Beyond the primary structural changes, the dynamic alterations in enzyme activity and related mRNA expression levels also show considerable variation across different studies. For example, the activity of pectinesterase (PE) in the granulated juice sacs of Kinnow mandarin is lower than that in healthy juice sacs.¹ Similarly, the activity of pectin methylesterase (PME) in the granulated juice sacs of the sweet orange cultivar "Itaborai" is lower than that in healthy juice sacs.¹⁷ In contrast, several transcriptomic studies have reported increased PME mRNA expression in the granulated juice sacs of late-ripening navel oranges¹⁸ and Huyou (*C. changshanensis*).⁷ In addition to PME, the activities of other enzymes involved in the synthesis and structural modification of cell wall polysaccharides also change during granulation. For instance, the activity of α -galactosidase and β -galactosidase increases two- to 3-fold in granulated juice sacs,¹⁹ while the enzyme activity and mRNA expression of polygalacturonase (PG) and cellulase (CL) decrease in granulated juice sacs.¹⁸ Clarifying the dynamic changes in the chemical structure of cell wall polysaccharides will help elucidate the roles of these enzymes and genes in juice sac granulation.

Until now, while the changes in the total amount of polysaccharide and the level of metabolic activity have been extensively studied, the detailed structural changes of polysaccharides during the granulation process are still not well understood. In this study, the polysaccharide composition of juice sacs was compared across different levels of granulation. Subsequently, water-soluble polysaccharides were fractionated by using DEAE-Sepharose chromatography. The structural

changes of each fraction of water-soluble polysaccharides were analyzed by using a combination of Fourier transform infrared (FT-IR) spectroscopy, nuclear magnetic resonance (NMR), and high-performance liquid chromatography (HPLC). This comprehensive approach is designed to reveal the detailed structural changes in water-soluble polysaccharides within the cell wall of granulated juice sacs.

2. MATERIALS AND METHODS

2.1. Sample Collection. Huyou (*C. changshanensis*) fruit were harvested at the ripening stage in December 2023 from an orchard in Quzhou City, Zhejiang Province, China. The juice sacs were collected and divided into four groups following the standard of the previous study according to their granulation level:¹⁸ healthy (H, with transparent appearance and juicy inside), gelatinous (G1, with the juice sac still transparent while semigellified inside), moderately granulated (G2, the juice sac was expanded, with cloudy white appearance and gellified inside), and severely granulated (G3, the juice sac was expanded, hard, with cloudy white or yellow appearance). The collected juice sacs were rapidly frozen with liquid nitrogen and freeze-dried. The dried samples were then ground into a fine powder and stored at -20°C for further analysis.

2.2. Fractionation and Quantitation of Cell Wall Polysaccharides. The alcohol-insoluble residue (AIR) was prepared with modifications based on the method described by Hwang.⁸ Fine powder of juice sacs (100 g) was mixed with 1 L of 95% (v/v) ethanol. The mixture was subjected to ultrasonic treatment in a water bath at room temperature for 30 min. The residue was collected by filtration through qualitative filter paper, and this process was repeated three times to ensure complete extraction. Subsequently, the collected residue was refluxed with 1 L of boiling 95% (v/v) ethanol for 3 h. After cooling to room temperature, the mixture was filtered to obtain the residue, which was then washed with ethanol. The excess ethanol was evaporated, and the residue was dried overnight in an oven at 60°C to yield the AIR. Three replicates were performed for each group, and the weight of the AIR was recorded.

Cell wall polysaccharide fractionation was performed according to the previously established method,²⁰ as illustrated in Figure 1. Initially, 10 g of AIR was stirred for 4 h at room temperature in 1 L of an aqueous

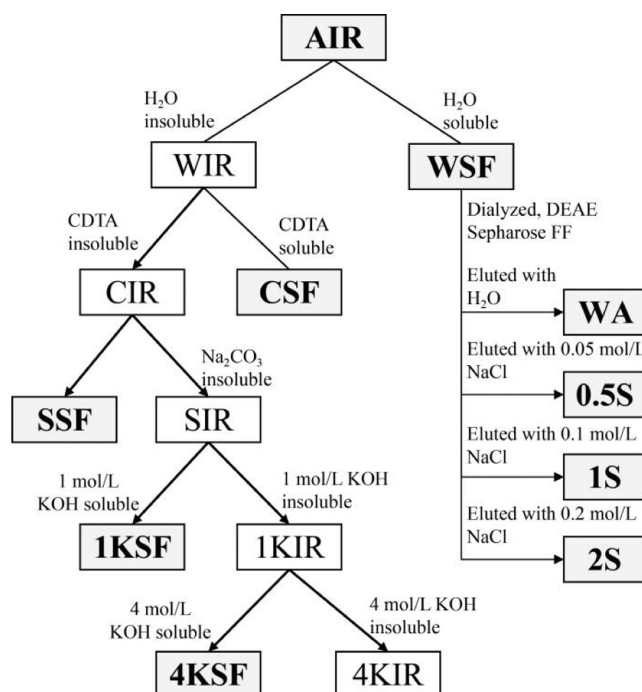


Figure 1. Scheme of cell wall polysaccharide fractionation.

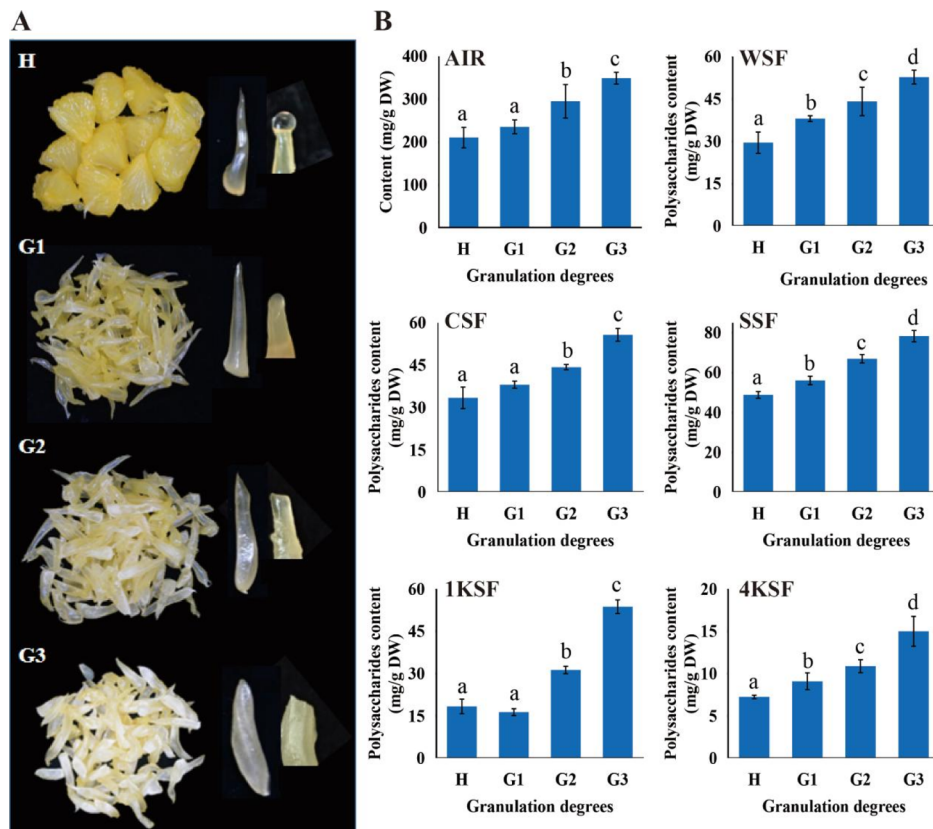


Figure 2. Contents of different polysaccharide fractions in juice sacs of different granulation degrees. (A) Appearance of juice sacs at different granulation degrees and (B) the contents of AIR and different polysaccharide fractions. Different lowercase letters represented significant differences at $p < 0.05$ level by Tukey testing.

solution containing 0.02% (w/v) thimerosal. The supernatant was recovered by centrifugation at 3900 rpm and designated as the water-soluble fraction (WSF). Subsequent sequential extractions were conducted on the remaining residue. First, it was extracted with 0.05 mol/L CDTA in 0.05 mol/L NaAcO/HAcO buffer (pH 6.0) containing 0.02% (w/v) thimerosal for 24 h, yielding the CDTA-soluble fraction (CSF). The residue was then extracted with 0.1 mol/L Na₂CO₃ in the presence of 0.1 mmol/L NaBH₄ for another 24 h, producing the Na₂CO₃-soluble fraction (SSF). Further extractions were performed using 1 mol/L KOH with 0.1% (w/v) NaBH₄ for 24 h (yielding the 1 mol/L KOH-soluble fraction, 1KSF) and 4 mol/L KOH with 0.1% (w/v) NaBH₄ for another 24 h (yielding the 4 mol/L KOH-soluble fraction, 4KSF). After each extraction step, the supernatant was recovered by centrifugation at 3900 rpm. For the 1KSF and 4KSF fractions, the pH was adjusted to 5.0 using glacial acetic acid. Three replicates were performed for each group. The total polysaccharide content in each fraction was determined using the phenol-sulfuric acid method.²¹

2.3. Fractionation and Quantitation of Water-Soluble Polysaccharides. For the fractionation of water-soluble polysaccharides, the lyophilized WSF was dissolved in ddH₂O at a concentration of 20 mg/mL and subjected to ion-exchange chromatography using a DEAE-Sepharose Fast Flow column (1.6 × 20 cm, GE Healthcare, Pittsburgh, PA, USA). The sample was eluted sequentially with ddH₂O, followed by 0.05, 0.1, 0.2, 0.3, and 0.4 mol/L NaCl solutions (each elution step consisted of 3 column bed volumes) at a flow rate of 0.5 mL/min. The eluent was collected in 4 mL fractions per tube (Figure 1).

The total polysaccharide content in each fraction was determined using the phenol-sulfuric acid method²¹ to generate the elution profile. Fractions corresponding to the same elution peak were pooled, concentrated at 45 °C, and dialyzed using dialysis bags with a molecular weight cutoff of 3000 Da to remove residual NaCl. The dialyzed

fractions were then concentrated under vacuum to obtain the purified water-soluble polysaccharide fractions.

These fractions were subsequently deproteinized using the Sevag reagent, following the method described by Shen et al.²² The deproteinized solution was reprecipitated in four volumes of anhydrous ethanol. The precipitates were collected and dried overnight in an oven at 60 °C to yield the final water-soluble polysaccharide fractions.

2.4. Characterization of Water-Soluble Polysaccharides Fractions. **2.4.1. Purity and Molecular Weight Assessment.** The polysaccharide content was determined using the phenol-sulfuric acid method.²¹ Phenolic and protein impurities within the polysaccharide fractions were assessed by analyzing the UV-visible spectrum of the samples (1 mg/mL) using a DU-8000 spectrophotometer (Beckman Coulter, Brea, CA, USA) over a wavelength range of 230–800 nm. Additionally, the total protein content in the polysaccharide fractions was quantified according to the instructions provided with the Bradford protein quantification kit (Beyotime Biotechnology, Jiangsu, China). The molecular weight and homogeneity of polysaccharides were analyzed by high-performance gel permeation chromatography (HPGPC) using a Waters S15 HPLC system equipped with a 2410 differential refractive index detector (Waters, Milford, MA, USA) coupled with a TSKgel G4000SWXL column (Tosoh, Japan), and the molecular weight was calculated according to the standard curve of dextran of average molecular weight of 556,000, 496,000, 289,000, 110,000, 63,300, 30,200, and 3050 Da.

2.4.2. Monosaccharide Composition. The monosaccharide composition of polysaccharides was analyzed using the method reported by Sun et al.²³ Specifically, 1 mg of polysaccharide sample was hydrolyzed with 1 mL of 2 mol/L trifluoroacetic acid (TFA) in a sealed container at 120 °C for 2 h. The hydrolyzed mixture was then evaporated by using rotary centrifugal evaporation at 30 °C to remove the solvent. The residue was subsequently washed multiple times with methanol to eliminate excess TFA and dissolved in 100 μL of deionized water

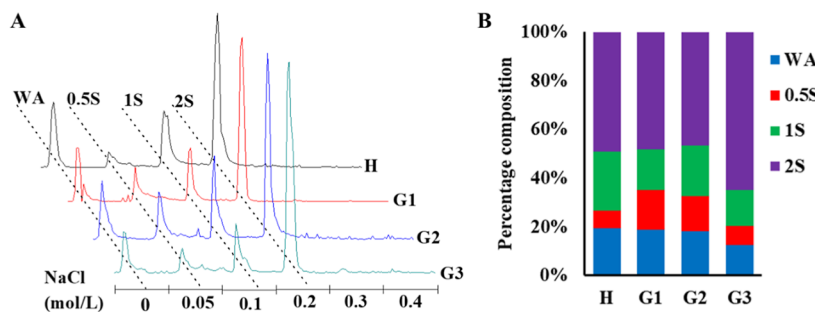


Figure 3. Composition of polysaccharide fractions in the WSFs. (A) Elution profiles of DEAE-Sepharose fast flow ion exchange chromatography and (B) the content ratio of different polysaccharide fractions. WA, water eluent; 0.5S, 0.05 mol/L NaCl eluent; 1S, 0.1 mol/L NaCl eluent; 2S, 0.2 mol/L NaCl eluent. The percentage composition was presented as the percentage of polysaccharide content in each fraction to the sum of all fractions.

(ddH₂O) for further derivatization. Each sample was processed in triplicate.

For precolumn derivatization, 100 μ L of the hydrolysate solution or monosaccharide standard solution was mixed with 120 μ L of a 0.5 mol/L methanol solution of 1-phenyl-3-methyl-5-pyrazolone and 100 μ L of a 0.3 mol/L NaOH solution. The mixture was incubated at 70 °C for 1 h. Subsequently, 100 μ L of a 0.3 mol/L HCl solution was added to neutralize the NaOH. Afterward, 1 mL of dichloromethane was added, and the mixture was vigorously shaken and centrifuged for 5 min. The supernatant, containing the labeled carbohydrates, was filtered through a 0.22 μ m membrane. A 10 μ L aliquot of the resulting solution was injected for HPLC analysis.

The HPLC analysis of the labeled monosaccharides was performed on a Waters 2695–2996 HPLC system (Waters, USA) equipped with a Sunfire C18 analytical column (4.6 \times 250 mm, 5 μ m, Waters, USA) maintained at a column temperature of 25 °C. The mobile phase consisted of a 0.1 mol/L KH₂PO₄ buffer (pH 6.7) (eluent A) and acetonitrile (eluent B). The gradient elution program is as follows: 0–30 min, 18% B; 30–60 min, linear gradient from 18% to 25% B; and 60–65 min, linear gradient from 25% to 18% B, with a flow rate of 1 mL/min. Detection was carried out at a wavelength of 245 nm. The monosaccharides were identified by comparing their retention times with those of the standards and quantified using a standard calibration curve.

2.4.3. FT-IR Analysis. FT-IR analysis was performed using a Nicolet iS10 Fourier Transform Infrared Spectrometer (Thermo Fisher Scientific, USA). For sample preparation, 1 mg of lyophilized polysaccharide was thoroughly mixed with potassium bromide (KBr) powder, ground, and then pressed into 1 mm pellets. The FT-IR spectra of the polysaccharides were recorded over a frequency range of 4000–400 cm^{-1} , with a resolution of 0.5 cm^{-1} and 32 scans per spectrum. The degree of methyl esterification (DM) was assessed based on the ratio of the peak area corresponding to esterified carboxyl groups to the combined peak areas of esterified and free carboxyl groups in the FT-IR spectra, as described by Du et al.²⁴

2.4.4. NMR Spectroscopy Analysis. For NMR spectroscopy, the lyophilized polysaccharide was dissolved in deuterated water (D₂O) to a final concentration of 40 mg/mL. The ¹H- and ¹³C NMR spectra were acquired using a JEOL JNM-ECZ500R/M1 500 MHz NMR spectrometer (JEOL, Japan). The ¹H NMR spectra were recorded at 25 °C after 256 scans, while the ¹³C NMR spectra were obtained at the same temperature after 10,240 scans. Chemical shifts were reported in parts per million (ppm). Data analysis was performed using MestRe Nova 9.0.1 software (Mestrelab Research SL, Spain). The glycosidic linkages in the samples were identified by comparing their chemical shifts with those reported in the literature as well as with authentic standards, including 1,4-galactan from lupines, arabinogalactan from larch, 1,4-galacturonans, and arabinan (Yuanye Bio-Technology Co., Ltd., China).

2.5. Rheological Analysis. The rheological properties of various water-soluble polysaccharide fractions, prepared at a concentration of 20 mg/mL, were evaluated using a DHR-1 rotational rheometer (TA Instruments, USA). The measurements were conducted with parallel

plates of 40 mm diameter and a gap of 1 mm. The viscosity of the samples was determined in the peak hold mode at a shear rate of 100 s⁻¹ and a temperature of 25 °C.

2.6. Statistical Analysis. The data were subjected to statistical analysis using one-way ANOVA with SPSS software (version 20.0, SPSS Inc., USA). Multiple comparisons between groups were conducted using the Tukey's honestly significant difference test. Results are presented as the mean \pm the standard deviation.

3. RESULTS

3.1. Composition of Polysaccharides in Juice Sacs at Different Granulation Levels. As granulation progresses, the juice sacs gradually lose their transparency and become increasingly harder and paler (Figure 2A). Concurrently, the content of AIR significantly increased, rising from 210.39 \pm 23.86 mg/g dry weight (DW) in healthy juice sacs to 348.86 \pm 13.66 mg/g DW in juice sacs at the G3 granulation stage. In parallel, the polysaccharide content in various fractions (WSF, CSF, SSE, 1KSF, and 4KSF) also increased with the progression of granulation (Figure 2B).

3.2. Composition of Water-Soluble Polysaccharide Fractions in Juice Sacs at Different Granulation Levels. The WSF was further purified and fractionated by using DEAE-Sepharose chromatography. Four polysaccharide fractions were obtained by eluting with water (WA), 0.05 mol/L (0.5S), 0.1 mol/L (1S), and 0.2 mol/L (2S) NaCl solutions, respectively. No polysaccharides were obtained from the 0.3 and 0.4 mol/L solutions (Figure 3A). Among these fractions, the 2S fraction accounted for the highest proportion of WSF. The absolute polysaccharide contents of all the fractions (WA, 0.5S, 1S, and 2S) in the juice sac were increasing with the progression of granulation, with the 2S fraction showing the most significant increase (Supporting Information, Table S1). However, the relative proportions of these fractions in the WSF varied depending on the degree of granulation. In the G1 and G2 samples, the proportion of the 0.5S fraction significantly increased, while the 1S fraction slightly decreased. In contrast, the G3 sample exhibited a significant increase in the 2S fraction and a decrease in the WA fraction (Figure 3B).

Following DEAE-Sepharose chromatography and subsequent deproteinization treatments, the majority of impurities, including phenolics and proteins, were effectively removed, as evidenced by the UV-visible spectrum (Supporting Information, Figure S1). However, the polysaccharide concentration of the WA fractions remained relatively low, ranging from 9.97% to 15.97%. This low concentration, coupled with the presence of unknown impurities, rendered these fractions unsuitable for further structural analysis. In contrast, the purity of the other water-soluble polysaccharide fractions exceeded 50% (Support-

ing Information, Figure S2), and these fractions were thus selected for subsequent detailed structural analysis.

The molecular weight distribution and homogeneity of these fractions were analyzed by HPGPC. As shown in the spectrum, the 2S fraction exhibited good uniformity and a tendency to increase in molecular weight. Specifically, it increased from 90,327 Da in the H sample to 119,714, 167,846, and 186,726 Da in the G1, G2, and G3 samples, respectively. In contrast, the 0.5S and 1S fractions were nonuniform, the molecular weight of the major component of 0.5S fraction tend to decrease, from 3411 Da in the H sample decreased to 3151, 3005, and 1776 Da in the G1, G2, and G3 samples, respectively. The molecular weight of the major component of the 1S fraction decreased slightly in the G1 and G2 samples and then increased significantly in the G3 sample (Supporting Information, Figure S3).

3.3. Primary Structure of Different Water-Soluble Polysaccharide Fractions. **3.3.1. Monosaccharide Composition.** The monosaccharide composition of the water-soluble polysaccharide fractions was analyzed and compared, with the results presented in Figure 4. A comprehensive profile of

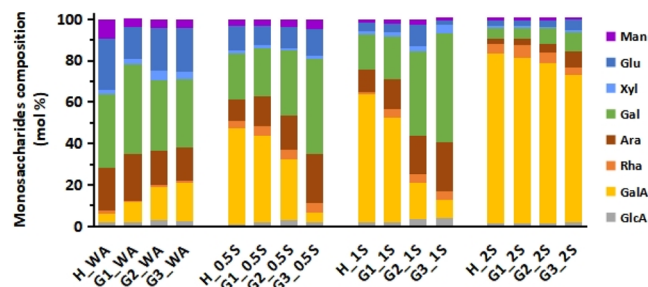


Figure 4. Monosaccharide composition of different water-soluble polysaccharide fractions from juice sacs of different granulation levels. Man, mannose; Glu, glucose; Xyl, xylose; Gal, galactose; Ara, arabinose; Rha, rhamnose; GalA, galacturonic acid; and GlcA, glucuronic acid.

monosaccharides was identified across all fractions, including seven neutral monosaccharides (mannose, rhamnose, glucose, galactose, xylose, arabinose, and trace amount of fucose) and two uronic acids (glucuronic acid and galacturonic acid).

In the WA fractions of all samples, neutral monosaccharides were the predominant components, accounting for 79.21% to 93.72% of the total monosaccharides. Among these, galactose (32.65% to 43.12%), arabinose (16.14% to 23.07%), and glucose (15.62% to 24.78%) were the most abundant monosaccharides. The proportion of galacturonic acid increased with the NaCl concentration in the eluent. Specifically, in the fractions eluted with 0.2 mol/L NaCl, galacturonic acid became the dominant monosaccharide, accounting for 71.11% to 81.70% of the total monosaccharides across different samples (Table 1).

As granulation progressed, the monosaccharide composition of the water-soluble polysaccharides gradually changed. In the WA fraction, the proportions of galacturonic acid and xylose consistently increased with granulation, while the proportions of arabinose, galactose, and mannose tended to decrease. The 0.5S and 1S fractions exhibit similar trends, which are somewhat contrary to those observed in the WA fraction. Specifically, in these fractions, the proportion of galacturonic acid decreased, while the proportions of rhamnose, arabinose, galactose, and mannose increased continuously with granulation. In the G2 and G3 juice sacs, the combined proportions of these four monosaccharides exceeded 50%. In the 2S fraction, there is a slight decrease in the proportions of galacturonic acid and

rhamnose, while the proportions of arabinose, galactose, and mannose continue to increase with the progression of granulation. The proportion of glucose remained stable in the progression of granulation (Figure 4).

Galacturonic acid and rhamnose are the primary structural components of the pectin backbone, which can be divided into two main regions: homogalacturonans (HG) and rhamnogalacturonans I (RG-I). The HG region consisted of a linear chain of covalently linked $\rightarrow 4$ - α -D-galactopyranosyluronic acid-(1 \rightarrow units, which are partially methyl-esterified at the C6 position and acetylated at O-2 or O-3.²⁵ The RG-I region was characterized by repeating units of $[\rightarrow 4]$ - α -D-galactopyranosyluronic acid-(1 \rightarrow 2)- α -L-rhamnopyranose-(1 \rightarrow], with side chains of galactans, arabinans, and/or arabinogalactans attached to the O-4 position of rhamnose.²⁵ The relative proportion of the RG-I region can be estimated by summing the molar percentages of rhamnose, galactose, and arabinose (2rhamnose mol % + galactose mol % + arabinose mol %), as described by Hu et al.²⁶ The extent of branching in the RG-I region can be indicated by the molar ratio of (galactose + arabinose)/rhamnose. For linear side chains, this ratio reflects the length of the side chain, while for nonlinear side chains, the galactose/arabinose/rhamnose ratio indicates the amount of galactose and arabinose per side chain. A higher molar ratio of (galactose + arabinose)/rhamnose suggests that the RG-I region has a longer or more branched structure.²⁷

The proportion of the RG-I domain (2 rhamnose mol % + galactose mol % + arabinose mol %) significantly increased with the progression of granulation, particularly in the 0.5S and 1S fractions. These fractions saw a substantial rise from 40.09% and 29.52% in healthy juice sacs to 78.54% and 84.64% in G3 juice sacs, respectively. Correspondingly, the HG domain decreased as the granulation advanced. The molar ratio of (galactose + arabinose)/rhamnose ratios in the 0.5S, 1S, and 2S fractions also increased in G2 and G3 juice sacs, indicating the elongation of RG-I side chains in the granulated juice sacs (Table 1). Overall, it can be concluded that with the progression of granulation, the water-soluble polysaccharides in the juice sacs exhibited an increase in both the RG-I domain and the length of arabinogalactan side chains.

3.3.2. Fourier Transform Infrared. FT-IR analysis was employed to detect variations in the typical groups of polysaccharides among different samples. However, the WA fractions were excluded from this analysis due to their low purity, which precluded the generation of reliable FT-IR spectra.

As illustrated in Figure 5A, the spectra of all tested fractions closely resembled those of the previously studied citrus pectins. The broad peak at around 3405 cm⁻¹ was assigned to the stretching vibration of the O-H bonds. The signals at 1407 cm⁻¹ and 2935 cm⁻¹ were assigned to the C-H bending vibration and C-H stretching vibration of polysaccharides, respectively. The spectral region between 800 cm⁻¹ and 1200 cm⁻¹, often referred to as the “fingerprint” region, exhibited unique characteristics for different polysaccharides²⁸ and was thus challenging to interpret in detail. Nonetheless, the tested fractions displayed similar spectral features in these regions.

The signals at 1637 cm⁻¹ and 1745 cm⁻¹ were assigned to the asymmetric stretching vibrations of nonesterified carbonyl C=O (COO⁻) and esterified carbonyl C=O (COO-R), respectively. Consequently, the DM was calculated as the ratio of the peak area at 1745 cm⁻¹ to the sum of the peak areas at 1637 cm⁻¹ and 1745 cm⁻¹.^{24,29-31} The DM of the 0.5S and 1S fractions decreased with the progression of granulation, while

Table 1. Chemical Composition of Polysaccharide Fractions from Juice Sacs in Different Granulation Degrees

fraction		monosaccharides (mol %)						GlcA	GalA
	Man	Rha	Glu	Gal	Xyl	Ara	Fuc		2Rha + Ara + Gal ^a
H_WA	9.28 ± 1.70	1.45 ± 0.75	24.78 ± 2.58	35.62 ± 2.67	2.31 ± 0.21	20.29 ± 1.87	trace	2.00 ± 0.09	4.27 ± 0.49
G1_WA	3.68 ± 0.31*	0.51 ± 0.07	15.62 ± 0.43*	43.12 ± 2.80*	2.70 ± 0.62	23.07 ± 2.80*	trace	2.16 ± 0.32	9.31 ± 4.54
G2_WA	4.02 ± 0.50*	1.13 ± 0.62	20.98 ± 1.17	34.23 ± 2.31	4.28 ± 0.26*	16.31 ± 0.51*	trace	2.86 ± 0.98	16.20 ± 1.60*
G3_WA	4.26 ± 0.45*	1.31 ± 1.03	21.01 ± 2.05	32.65 ± 2.44	3.82 ± 0.63*	16.14 ± 0.86*	trace	2.28 ± 0.35	18.51 ± 2.57*
H_0.5S	3.29 ± 0.65	3.66 ± 0.77	11.84 ± 6.42	22.21 ± 5.67	1.39 ± 0.43	10.56 ± 1.75	trace	1.11 ± 0.26	45.93 ± 13.89
G1_0.5S	3.09 ± 0.03	4.80 ± 1.17	9.53 ± 0.58	22.95 ± 2.31	1.51 ± 0.49	14.42 ± 1.28*	trace	1.94 ± 0.10	41.77 ± 4.71
G2_0.5S	3.67 ± 1.31	4.41 ± 0.70	10.13 ± 1.04	31.14 ± 16.25	1.35 ± 0.30	16.97 ± 5.18*	trace	2.81 ± 0.27*	29.52 ± 23.13
G3_0.5S	4.98 ± 2.23	4.31 ± 1.70	12.78 ± 7.94	45.82 ± 5.59*	1.30 ± 0.34	24.10 ± 4.16*	trace	2.08 ± 0.54*	78.54 ± 6.36*
H_1S	1.57 ± 0.70	0.94 ± 0.43	4.25 ± 1.50	16.73 ± 9.55	1.58 ± 0.07	10.91 ± 8.51	trace	2.07 ± 0.76	61.95 ± 16.40
G1_1S	1.98 ± 0.05	4.19 ± 1.41*	4.55 ± 0.33	20.77 ± 1.42	1.82 ± 0.36	14.43 ± 2.17	trace	2.11 ± 0.24	50.15 ± 5.21
G2_1S	2.70 ± 0.37*	3.82 ± 0.15*	10.27 ± 3.44*	40.45 ± 1.82*	2.86 ± 0.59*	18.73 ± 2.93	trace	3.46 ± 0.45	17.72 ± 1.53*
G3_1S	0.59 ± 0.09*	4.12 ± 0.45*	2.26 ± 1.14	52.31 ± 0.61*	4.03 ± 0.58*	24.09 ± 1.80*	trace	4.07 ± 0.68*	8.54 ± 1.18*
H_2S	0.47 ± 0.17	4.62 ± 2.14	2.94 ± 0.72	4.93 ± 0.99	0.80 ± 0.21	3.00 ± 1.05	trace	1.53 ± 0.29	81.70 ± 5.45
G1_2S	0.58 ± 0.07	6.18 ± 1.20	2.66 ± 0.41	5.20 ± 0.10	1.01 ± 0.24	3.15 ± 0.64	trace	1.52 ± 0.20	79.70 ± 2.04
G2_2S	0.69 ± 0.13	4.87 ± 1.34	2.91 ± 0.42	7.83 ± 1.95	0.77 ± 0.07	4.04 ± 1.44	trace	1.49 ± 0.21	77.40 ± 5.19
G3_2S	0.22 ± 0.07	3.65 ± 0.83	4.90 ± 0.87	9.30 ± 7.15	1.16 ± 0.03*	7.77 ± 2.32*	trace	1.91 ± 0.59	71.11 ± 11.21

^aRG-1% = 2Rha % + Ara % + Gal %. Values represent means ± standard derivatives of three replicates; values with * indicate significant difference ($p < 0.05$) compared with the healthy juice sac (H) in WA, 0.05 mol/L NaCl eluent (0.5S), 0.1 mol/L NaCl eluent (1S), and 0.2 mol/L NaCl eluent (2S), respectively.

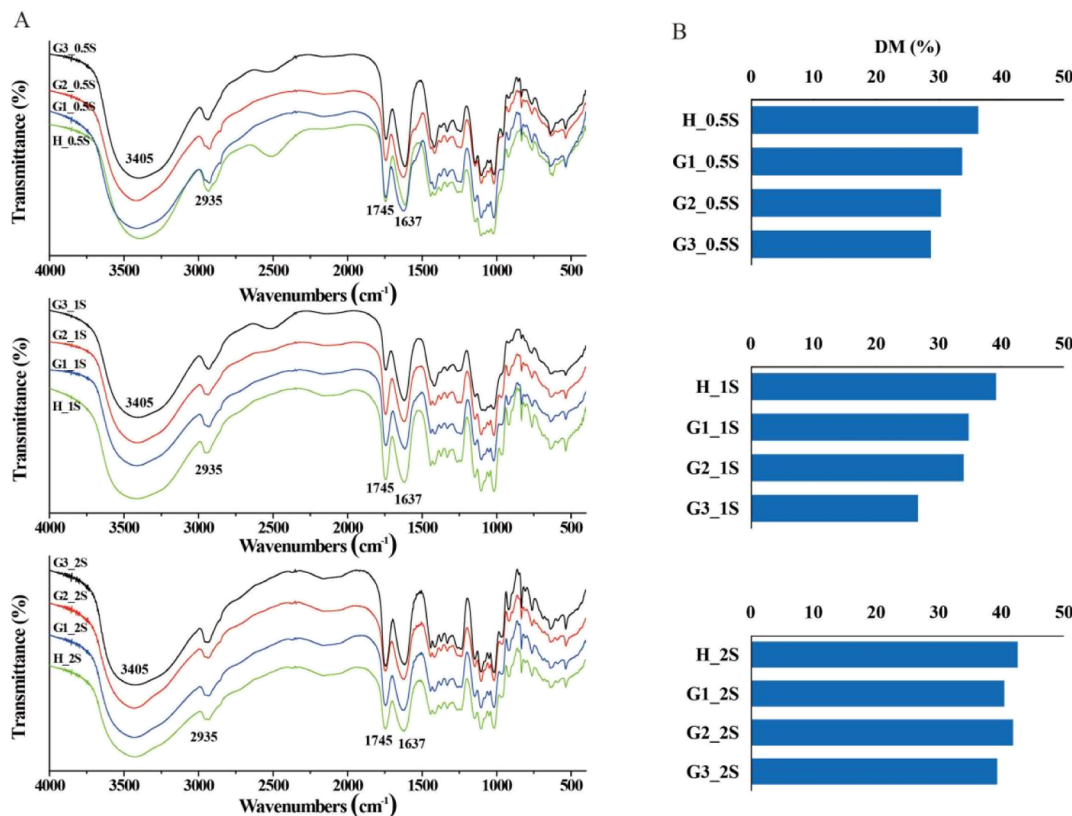


Figure 5. FT-IR spectrum (A) and the degree of methyl esterification (DM) (B) of water-soluble polysaccharide fractions.

that of the 2S fraction remained stable (Figure 5B). These findings suggest that demethylesterification of polygalacturonic acid occurs during the granulation process.

3.3.3. NMR. NMR spectroscopy was employed to confirm and elucidate the structural features of different polysaccharide fractions. By the combination of the ¹H and ¹³C NMR spectra, the signals corresponding to galacturonic acid, rhamnose, arabinose, and galactose were identified (Figure 6A–F, Table 2).

Galacturonic acid was partially methyl-esterified at the C6 position and predominantly linked in the form of →4)- α -D-galactopyranosyluronate-(1→ units (1,4-6MeGalA). The characteristic chemical shifts are assigned as follows: C1 at δ 100.56 ppm, C2 at δ 67.79 ppm, C3 at δ 68.02 ppm, C4 at δ 79.12 ppm, C5 at δ 70.57 ppm, C6 at δ 170.92 ppm, and the methyl ester group ($-\text{OCH}_3$) at δ 52.97 ppm. Nonesterified GalA exhibited peaks at C1 (δ 99.06 ppm), C2 (δ 68.91 ppm), C3 (δ 68.20 ppm), C4 (δ 77.99 ppm), C5 (δ 71.37 ppm), and C6 (175.50 ppm), as verified against an authentic standard of 1,4-GalA and the results of previous studies.³²

Rhamnose was identified as being linked in the form of →2)- α -L-rhamnopyranose-(1→, with side chains attached to the O-4 position. The signals for C1, C3, C5, and C6 were successfully identified by comparison with the results of previous studies.^{32,33} The signals of H1 (δ 1.16 ppm) and H6 (δ 5.16 ppm) of rhamnose were also found in the ¹H NMR spectra³³ (Figure 6).

Arabinose was found to be linked in various forms, including 1,5-, 1,3-, 1,3,5-, and 1-linkages, as confirmed by comparison with an authentic arabinan standard and the results of previous studies.^{32,34,35} Galactose was linked in 1,3-, 1,6-, and 1-linkages, as verified against an authentic arabinogalactan standard from larch and the results of previous studies.^{32,35–37} No signal of 1,4-

galactan was detected when compared with an authentic 1,4-galactan standard. Thus, it was deduced that the arabinose existed as arabinan and arabinogalactan and that the galactose existed as arabinogalactans in the side chain. The ¹H NMR spectra of arabinan and arabinogalactan were observed in the δ 3.44–5.15 ppm region³³ (Figure 6). The ¹H and ¹³C NMR spectra revealed significant structural changes in the polysaccharides of granulated samples compared with healthy samples, particularly in the 0.5S and 1S fractions.

In the 0.5S fraction, the sample from healthy juice sacs was primarily composed of 1,4-6MeGalA (methyl-esterified galacturonic acid). As granulation progressed, the peaks corresponding to 1,4-6MeGalA gradually diminished in prominence. Conversely, the relative abundance of 1,4-GalA (nonesterified galacturonic acid) increased slightly, becoming detectable in the G2 sample and further elevated in the G3 sample. Additionally, the peak signals for rhamnose, arabinose, and galactose intensified in the G2 sample and became dominant in the G3 sample (Figure 6). This trend indicated an increase in the RG-I region and the branching side chains, which was consistent with the results of the monosaccharide molar proportion analysis by HPLC (Figure 4).

In the 1S fraction, trends similar to those observed in the 0.5S fraction were noted (Figure 6). In contrast, the 2S fraction was predominantly characterized by 1,4-6MeGalA in both healthy and granulated samples. However, a slight decrease in the 1,4-6MeGalA signals was observed in the granulated samples, accompanied by a modest increase in the signals corresponding to 1,4-GalA, arabinans, and arabinogalactans.

3.4. Rheological Properties of Different Water-Soluble Polysaccharide Fractions in Juice Sacs of Different Granulation Levels. To further elucidate how structural

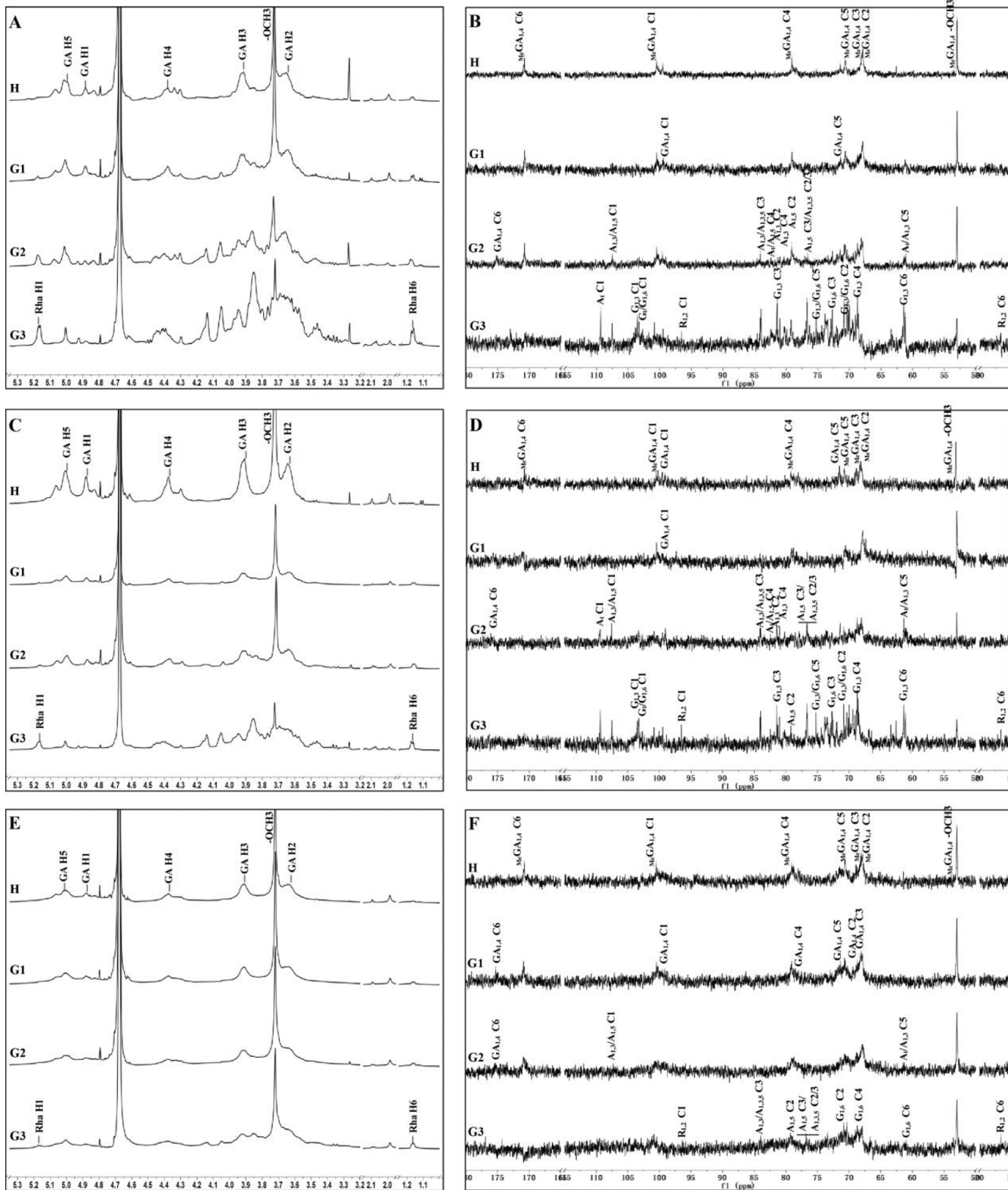


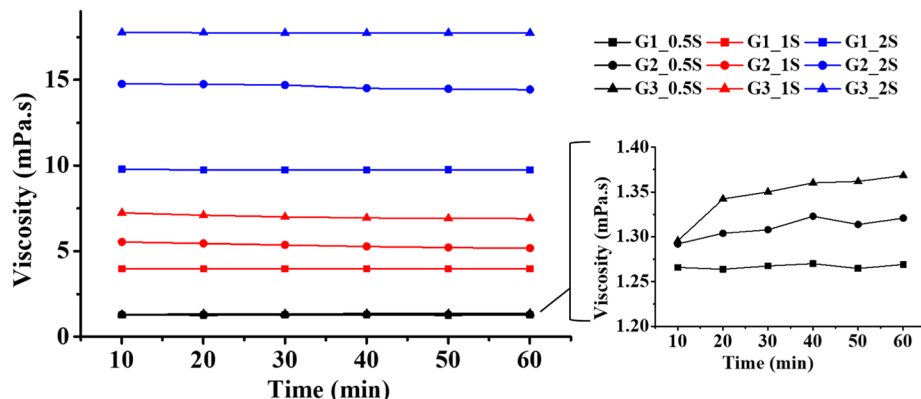
Figure 6. NMR spectrum of water-soluble polysaccharide fractions. (A) ¹H NMR of 0.5S fraction; (B) ¹³C NMR of 0.5S fraction; (C) ¹H NMR of 1S fraction; (D) ¹³C NMR of 1S fraction; (E) ¹H NMR of 2S fraction; and (F) ¹³C NMR of 2S fraction.

changes influence the physical properties of water-soluble polysaccharides, a rheological analysis was conducted on various fractions, excluding the WA fractions. Polysaccharide fractions derived from granulated juice sacs exhibited higher viscosity compared with those from healthy juice sacs. Overall, fractions

eluted with higher concentrations of NaCl demonstrated greater viscosity than those eluted with lower NaCl concentrations (Figure 7).

Table 2. ^{13}C NMR Spectral Assignments of Polysaccharide Fractions from Juice Sacs in Different Granulation Degrees (500 MHz)

	notation	C1	C2	C3	C4	C5	C6	-OCH3
$\rightarrow 4\text{-}\alpha\text{-D-6MeGalAp-(1\mathord{\rightarrow} 4)}$	$\text{MeGA}_{1,4}$	100.56	67.79	68.02	79.12	70.57	170.92	52.97
$\rightarrow 4\text{-}\alpha\text{-D-GalAp-(1\mathord{\rightarrow} 4)}$	$\text{GA}_{1,4}$	99.06	68.91	68.20	77.99	71.37	175.50	
$\rightarrow 2\text{-}\alpha\text{-L-Rhap-(1\mathord{\rightarrow} 2)}$	$\text{Rha}_{1,2}$	96.55		73.81		69.44	16.60	
$\rightarrow 2,4\text{-}\alpha\text{-L-Rhap-(1\mathord{\rightarrow} 2,4)}$	$\text{Rha}_{1,2,4}$	96.55		73.81		70.08	16.68	
$\alpha\text{-Araf-(1\mathord{\rightarrow} 6)}$	A_t	109.33	81.35	76.64	82.33	61.18		
$\rightarrow 5\text{-}\alpha\text{-L-Araf-(1\mathord{\rightarrow} 5)}$	$\text{A}_{1,5}$	107.54	79.21	76.64	82.33	66.29		
$\rightarrow 3,5\text{-}\alpha\text{-L-Araf-(1\mathord{\rightarrow} 3,5)}$	$\text{A}_{1,3,5}$	107.54	76.64	83.98	81.35	66.58		
$\rightarrow 3\text{-}\alpha\text{-L-Araf-(1\mathord{\rightarrow} 3)}$	$\text{A}_{1,3}$	107.54	81.35	83.98	80.93	61.18		
$\rightarrow 6\text{-}\beta\text{-Galp-(1\mathord{\rightarrow} 6)}$	$\text{G}_{1,6}$	103.23	70.87	73.84	68.75	75.24	69.52	
$\rightarrow 3\text{-}\beta\text{-Galp-(1\mathord{\rightarrow} 3)}$	$\text{G}_{1,3}$	103.46	70.87	81.44	68.75	75.24	61.18	
$\rightarrow\beta\text{-Galp-(1\mathord{\rightarrow} 1)}$	G_t	103.23	70.26	70.49	73.68	70.26	61.37	

**Figure 7.** Rheological characteristics of different water-soluble polysaccharide fractions.

4. DISCUSSION

Based on the results presented above, it can be concluded that both the increase in content and the structural modifications of cell wall polysaccharides are associated with the granulation process in citrus juice sacs.

In terms of the content of cell wall polysaccharides, this study observed that the contents of WSF, CSF, and SSF increased with the progression of granulation. These findings are consistent with the results reported by Yan et al.¹³ and Li et al.¹⁴ Additionally, the 1KSF and 4KSF, which have been previously identified as primarily consisting of hemicellulose and pectin anchored in the cellulose load-bearing network,^{38,39} also exhibited increased levels with granulation progression. Therefore, these results align with both prior chemical quantification studies and in situ labeling of cell wall components, supporting the conclusion that juice sac granulation is characterized by cell wall thickening due to polysaccharide accumulation.⁷

One of the structural changes observed in water-soluble polysaccharides during granulation was the decrease in the methyl esterification level of galacturonic acid in the granulated juice sacs. This finding was supported by both FT-IR and NMR analyses. It aligns with previous research using chemical reaction methods, which demonstrated a reduction in the esterification degree of water-soluble and EDTA-soluble polysaccharides in the granulated juice sacs of Sanbokan (*Citrus sulcata* hort. ex Takahashi).¹⁵ This result is also consistent with several studies that reported elevated mRNA expression of PME in the granulated juice sacs of various citrus species, including navel orange (*Citrus sinensis* Osbeck), Huyou (*C. changshanensis*), Harumi tangor, and "Dayagan" hybrid citrus.^{7,10,13,18,40} PME

catalyzes the demethylesterification of pectin, suggesting that it may be a crucial target for inhibiting granulation. The decrease in esterification leads to an increase in the gelatinous degree⁴¹ and a reduction in the elastic properties of pectin.⁴² These changes are likely contributors to the altered texture of the juice sac during granulation.

Another significant structural change observed in water-soluble polysaccharides was in their monosaccharide composition. The water-soluble polysaccharides from granulated juice sacs exhibited substantial increases in the molar proportions of rhamnose, arabinose, galactose, and mannose. A previous study reported that WSP from granulated or collapsed juice sacs of "Marsh Seedless" grapefruit was characterized by elevated levels of neutral sugars, including rhamnose, fucose, arabinose, xylose, mannose, galactose, and glucose.⁸ Our findings are in partial agreement with those in this earlier study.

In conjunction with the increased proportion of neutral sugars, the primary structure of water-soluble polysaccharides in the granulated juice sacs underwent significant changes. The water-soluble polysaccharides in granulated juice sacs were characterized by an increased RG-I region and a decreased HG region. Additionally, the polysaccharide chains exhibited increased branching, with both the number and length of arabinogalactan, arabinan, and galactan side chains being elevated. These findings are consistent with those of Li et al.,¹⁴ who used AFM to observe that granulated juice sacs contained a larger amount of long-chain and highly branched water-soluble polysaccharides. Longer side chains have been associated with increased entanglements between pectin molecules, and a higher number of side chains have been shown to enhance pectin gel strength.⁴³ In previous studies

comparing cell wall polysaccharides among different citrus cultivars, higher RG-I regions and multibranched side chains were found in cultivars with inferior mastication traits. These structural features are believed to enhance intercellular adhesion by cross-linking more pectin side chains with other cell wall matrix components, thereby forming a more stable network of cell wall polysaccharides.⁴⁴ Therefore, it can be inferred that the increased RG-I region and the increased number and length of side chains may contribute to the inferior mastication traits observed in the granulated juice sacs. The viscosity of water-soluble polysaccharides is influenced by several factors, including molecular weight,⁴⁵ DM,⁴² and the amount of side chains.⁴³ In the present study, the increased viscosity observed in the 0.5S, 1S, and 2S fractions from granulated juice sacs may be attributed to the higher amount of side chains. This conclusion is supported by previous findings that an increased number of side chains enhances pectin gel strength.⁴³

In our previous study, transcriptome data revealed that numerous genes involved in the structural changes of cell wall polysaccharides were upregulated in granulated juice sacs. These genes encoded enzymes such as polygalacturonase, pectinesterase, pectate lyase, and xyloglucan galactosyltransferase.⁷ However, the specific roles that these genes play in the granulation remain unclear. PME has been implicated in low-temperature-induced juice sac granulation in navel oranges.^{18,40} Beyond PME, other enzymes and molecules that potentially contribute to the elongation of arabinan/arabinogalactan branches or the increase of the RG-I region of polysaccharides remain to be identified. Given the observed structural changes in cell wall polysaccharides, we infer that a complex array of molecular mechanisms likely underlie these changes during granulation. The results of the present study suggest that elucidating the molecular mechanisms of cell wall polysaccharide structural modifications is crucial for understanding the biological mechanisms underlying citrus granulation.

In summary, the present study uncovered several structural changes in the water-soluble polysaccharides of granulated citrus juice sacs compared to the healthy ones. Notable findings included the decrease in the DM in the HG region, the significant increase in the RG-I regions, and the substantial increase in the branching side chains of RG-I, composed of arabinans and arabinogalactans, with the progression of granulation. By shedding light on these structural alterations, our study provides a biochemical foundation for further investigation into the molecular mechanisms underlying cell wall polysaccharide modifications.

ASSOCIATED CONTENT

Supporting Information

The Supporting Information is available free of charge at <https://pubs.acs.org/doi/10.1021/acs.jafc.Sc05802>.

Contents of different water-soluble polysaccharide fractions in the juice sacs; UV-visible spectrum of different water-soluble polysaccharide fractions; contents of polysaccharides in different water-soluble polysaccharide fractions; and HPGC spectrum of different water-soluble polysaccharide fractions ([PDF](#))

AUTHOR INFORMATION

Corresponding Author

Jiping Cao — Zhejiang Key Laboratory of Horticultural Crop Quality Improvement/Horticultural Products Cold Chain

Logistics Technology and Equipment National-Local Joint Engineering Laboratory, Zhejiang University, Hangzhou 310058, PR China; Hainan Institute of Zhejiang University, Sanya 572025, PR China;  orcid.org/0000-0003-0840-5590; Phone: +86 571 88982229; Email: 0017165@zju.edu.cn

Authors

Xuemin Zhang — Zhejiang Key Laboratory of Horticultural Crop Quality Improvement/Horticultural Products Cold Chain Logistics Technology and Equipment National-Local Joint Engineering Laboratory, Zhejiang University, Hangzhou 310058, PR China

Xuanang Zheng — Zhejiang Key Laboratory of Horticultural Crop Quality Improvement/Horticultural Products Cold Chain Logistics Technology and Equipment National-Local Joint Engineering Laboratory, Zhejiang University, Hangzhou 310058, PR China

Haojie Wang — Zhejiang Key Laboratory of Horticultural Crop Quality Improvement/Horticultural Products Cold Chain Logistics Technology and Equipment National-Local Joint Engineering Laboratory, Zhejiang University, Hangzhou 310058, PR China

Chen Kang — Zhejiang Key Laboratory of Horticultural Crop Quality Improvement/Horticultural Products Cold Chain Logistics Technology and Equipment National-Local Joint Engineering Laboratory, Zhejiang University, Hangzhou 310058, PR China

Rong Jin — Zhejiang Key Laboratory of Horticultural Crop Quality Improvement/Horticultural Products Cold Chain Logistics Technology and Equipment National-Local Joint Engineering Laboratory, Zhejiang University, Hangzhou 310058, PR China

Dengliang Wang — Institute of Fruit Tree Research, Quzhou Academy of Agricultural and Forestry Science, Quzhou 324000, PR China

Shaojia Li — Zhejiang Key Laboratory of Horticultural Crop Quality Improvement/Horticultural Products Cold Chain Logistics Technology and Equipment National-Local Joint Engineering Laboratory, Zhejiang University, Hangzhou 310058, PR China

Yue Wang — Zhejiang Key Laboratory of Horticultural Crop Quality Improvement/Horticultural Products Cold Chain Logistics Technology and Equipment National-Local Joint Engineering Laboratory, Zhejiang University, Hangzhou 310058, PR China

Bo Zhang — Zhejiang Key Laboratory of Horticultural Crop Quality Improvement/Horticultural Products Cold Chain Logistics Technology and Equipment National-Local Joint Engineering Laboratory, Zhejiang University, Hangzhou 310058, PR China;  orcid.org/0000-0001-8181-9111

Chongde Sun — Zhejiang Key Laboratory of Horticultural Crop Quality Improvement/Horticultural Products Cold Chain Logistics Technology and Equipment National-Local Joint Engineering Laboratory, Zhejiang University, Hangzhou 310058, PR China; Hainan Institute of Zhejiang University, Sanya 572025, PR China;  orcid.org/0000-0002-2874-0292

Complete contact information is available at:

<https://pubs.acs.org/10.1021/acs.jafc.Sc05802>

Notes

The authors declare no competing financial interest.

ACKNOWLEDGMENTS

This work was supported by the National Key R&D Program of China (2024YFD2100101), the Agricultural Major Technology Collaborative Promotion Program of Zhejiang province (2024ZDXT04), the Hangzhou Key Project of Agricultural and Social Development (20231203A15), and the Fundamental Research Funds for the Central Universities (226-2023-00152). We thank Xiangli Kong from the Institute of Nuclear Agricultural Sciences of Zhejiang University for the support in rheological properties analysis. We thank Lijuan Mao and Jiaojiao Wang from the Analysis Center of Agrobiology and Environmental Sciences of Zhejiang University for their support in FT-IR detection and NMR detection, respectively.

REFERENCES

- (1) Sharma, R. R.; Saxena, S. K. Rootstocks influence granulation in Kinnow mandarin (*Citrus nobilis* × *C. deliciosa*). *Sci. Hortic.* **2004**, *101*, 235–242.
- (2) Sharma, R. R.; Singh, R.; Saxena, S. K. Characteristics of citrus fruits in relation to granulation. *Sci. Hortic.* **2006**, *111* (1), 91–96.
- (3) Chen, C. Y.; Nie, Z. P.; Wan, C. P.; Gan, Z. Y.; Chen, J. Y. Suppression on postharvest juice sac granulation and cell wall modification by chitosan treatment in harvested pummelo (*Citrus grandis* L. Osbeck) stored at room temperature. *Food Chem.* **2021**, *336*, 127636.
- (4) Cao, J. P.; Kang, C.; Chen, Y. Y.; Karim, N.; Wang, Y.; Sun, C. D. Physicochemical changes in *Citrus reticulata* cv. Shatangju fruit during vesicle collapse. *Postharvest Biol. Technol.* **2020**, *165*, 111180.
- (5) Kang, C.; Cao, J. P.; Wang, Y.; Sun, C. D. Advances of section drying in citrus fruit: The metabolic changes, mechanisms and prevention methods. *Food Chem.* **2022**, *395*, 133499.
- (6) Yao, S. X.; Wang, Z. M.; Cao, Q.; Xie, J.; Wang, X. R.; Zhang, R.; Deng, L. L.; Ming, J.; Zeng, K. F. Molecular basis of postharvest granulation in orange fruit revealed by metabolite, transcriptome and methylome profiling. *Postharvest Biol. Technol.* **2020**, *166*, 111205.
- (7) Kang, C.; Jiang, A. Z.; Yang, H.; Zheng, G. X.; Wang, Y.; Cao, J. P.; Sun, C. D. Integrated physicochemical, hormonal, and transcriptomic analysis revealed the underlying mechanisms for granulation in Huyou (*Citrus changshanensis*) fruit. *Front. Plant Sci.* **2022b**, *13*, 923443.
- (8) Hwang, Y. S.; Huber, D. J.; Albrigo, L. G. Comparison of cell wall components in normal and disordered juice vesicles of grapefruit. *J. Am. Soc. Hortic. Sci.* **1990**, *115* (2), 281–287.
- (9) Wu, J. L.; Pan, T. F.; Guo, Z. X.; Pan, D. M. Specific Lignin accumulation in granulated juice sacs of *Citrus maxima*. *J. Agric. Food Chem.* **2014**, *62*, 12082–12089.
- (10) Liu, Y. C.; Yan, D. D.; Hou, J.; Zhang, H. Y.; Wang, W.; Hong, M.; He, M. Y.; Yang, X. Z.; Zeng, K. F.; Yao, S. X. Hypothesis of cell wall metabolism disorder in segment drying: Evidence from vesicle collapse in 'Dayagan' hybrid citrus fruit. *Postharvest Biol. Technol.* **2023**, *204*, 112431.
- (11) Shi, M. Y.; Liu, X.; Zhang, H. P.; He, Z. Y.; Yang, H. B.; Chen, J. J.; Feng, J.; Yang, W. H.; Jiang, Y. W.; Yao, J. L.; Deng, C. H.; Xu, J. The IAA- and ABA-responsive transcription factor CgMYB58 upregulates lignin biosynthesis and triggers juice sac granulation in pummelo. *Hortic. Res.* **2020**, *7*, 139.
- (12) Liu, L. N.; Chen, Y. R.; Wu, W. L.; Chen, Q. Y.; Tian, Z. J.; Huang, J. K.; Ren, H. Q.; Zhang, J. C.; Du, X.; Zhuang, M. L.; Wang, P. A multilevel investigation to reveal the regulatory mechanism of lignin accumulation in juice sac granulation of pomelo. *BMC Plant Biol.* **2024**, *24*, 390.
- (13) Yan, D. D.; Liu, Y. C.; Hou, J.; Huang, M. Z.; Wang, W.; Xu, H. M.; Zeng, K. F.; Yao, S. X. Metabolic remodeling underlying citrus segment drying: Insights from lignin non-accumulating granulation in Harumi tangor vesicles. *Postharvest Biol. Technol.* **2024**, *211*, 112839.
- (14) Li, Q. Y.; Yao, S. X.; Deng, L. L.; Zeng, K. F. Changes in biochemical properties and pectin nanostructures of juice sacs during the granulation process of pomelo fruit (*Citrus grandis*). *Food Chem.* **2022a**, *376*, 131876.
- (15) Goto, A. Relationship between pectic substances and calcium in healthy, gelated, and granulated juice sacs of Sanbokan (*Citrus sulcata* hort. ex Takahashi) fruit. *Plant Cell Physiol.* **1989**, *30* (6), 801–806.
- (16) Sinclair, W. B.; Jolliffe, V. A. Chemical changes in the juice vesicles of granulated Valencia oranges. *J. Food Sci.* **1961**, *26* (3), 276–282.
- (17) Nayak, S. L.; Sethi, S.; Nain, L.; Dubey, A. K.; Chawla, G. Changes in microstructure, enzymatic activity and functional quality of citrus juice sacs upon granulation. *Natl. Acad. Sci. Lett.* **2023**, *46* (5), 439–443.
- (18) Wu, L. M.; Wang, C.; He, L. G.; Wang, Z. J.; Tong, Z.; Song, F.; Tu, J. F.; Qiu, W. M.; Liu, J. H.; Jiang, Y. C.; Peng, S. A. Transcriptome analysis unravels metabolic and molecular pathways related to fruit sac granulation in a late-ripening navel orange (*Citrus sinensis* Osbeck). *Plants* **2020**, *9* (1), 95.
- (19) Burns, J. K. Respiratory rates and glycosidase activities of juice vesicles associated with section-drying in citrus. *Hortscience* **1990**, *25* (5), 544–546.
- (20) Ponce, N. M. A.; Ziegler, V. H.; Stortz, C. A.; Sozzi, G. O. Compositional changes in cell wall polysaccharides from Japanese plum (*Prunus salicina* Lindl.) during growth and on-tree ripening. *J. Agric. Food Chem.* **2010**, *58*, 2562–2570.
- (21) Dubois, M.; Gilles, K. A.; Hamilton, J. K.; Rebers, P. A.; Smith, F. Colorimetric method for determination of sugars and related substances. *Anal. Chem.* **1956**, *28* (3), 350–356.
- (22) Shen, C. Y.; Yang, L.; Jiang, J. G.; Zheng, C. Y.; Zhu, W. Immune enhancement effects and extraction optimization of polysaccharides from *Citrus aurantium* L. var. amara Engl. *Food Funct.* **2017**, *8*, 796–807.
- (23) Sun, H. H.; Mao, W. J.; Chen, Y.; Guo, S. D.; Li, H. Y.; Qi, X. H.; Chen, Y. L.; Xu, J. Isolation, chemical characteristics and antioxidant properties of the polysaccharides from marine fungus *Penicillium* sp. F23–2. *Carbohydr. Polym.* **2009**, *78* (1), 117–124.
- (24) Du, Y. Y.; Zhang, S. K.; Waterhouse, G. I. N.; Zhou, T.; Xu, F. Z.; Wang, R. R.; Sun-Waterhouse, D. X.; Wu, P. High-intensity pulsed electric field-assisted acidic extraction of pectin from citrus peel: Physicochemical characteristics and emulsifying properties. *Food Hydrocolloids* **2024**, *146*, 109291.
- (25) Colodel, C.; Vriesmann, L. C.; Carmen Petkowicz, L. D. O. Cell wall polysaccharides from Ponkan mandarin (*Citrus reticulata* Blanco cv. Ponkan) peel. *Carbohydr. Polym.* **2018**, *195*, 120–127.
- (26) Hu, W.; Ye, X.; Chantapakul, T.; Chen, S.; Zheng, J. Manosonication extraction of RG-I pectic polysaccharides from citrus waste: Optimization and kinetics analysis. *Carbohydr. Polym.* **2020**, *235*, 115982.
- (27) Gu, J. Y.; Lin, L. Z.; Zhao, M. M. Highly branched rhamnogalacturonan-I type pectin from wolfberry: purification, characterization, and structure-prebiotic/immunomodulatory activity relationship. *J. Agric. Food Chem.* **2024**, *72*, 14022–14034.
- (28) Hosseini, S. S.; Khodaiyan, F.; Yarmand, M. S. Optimization of microwave assisted extraction of pectin from sour orange peel and its physicochemical properties. *Carbohydr. Polym.* **2016**, *140*, 59.
- (29) Szymanska-Charget, M.; Zdunek, A. Use of FT-IR spectra and PCA to the bulk characterization of Cell Wall residues of fruits and vegetables along a fraction process. *Food Biophys.* **2013**, *8*, 29–42.
- (30) Koziol, A.; Sroda-Pomianek, K.; Górnjak, A.; Wikiera, A.; Cyprych, K.; Malik, M. Structural determination of pectins by spectroscopy methods. *Coatings* **2022**, *12*, 546.
- (31) Zhao, J. Y.; Hong, T.; Hou, Y. J.; Song, X. X.; Yin, J. Y.; Geng, F.; Nie, S. P. Comparison of structures and emulsifying properties between water-extracted pectins from *Fructus aurantii*. *Int. J. Biol. Macromol.* **2023**, *242* (No), 125005.
- (32) Li, G.; Wang, F.; Wang, M. M.; Tang, M. T.; Zhou, T.; Gu, Q. Physicochemical, structural and rheological properties of pectin isolated from citrus canning processing water. *Int. J. Biol. Macromol.* **2022c**, *195*, 12–21.

- (33) Li, J. H.; Wang, L.; Yang, K.; Zhang, G. C.; Li, S.; Gong, H. J.; Liu, M. Q.; Dai, X. J. Structure characteristics of low molecular weight pectic polysaccharide and its anti-aging capability by modulating the intestinal homeostasis. *Carbohydr. Polym.* **2023**, *303*, 120467.
- (34) Shofiqur Rahman, A. K. M.; Kato, K.; Kawai, S.; Takamizawa, K. Substrate specificity of the α-L-arabinofuranosidase from *Rhizomucor pusillus* HHT-1. *Carbohydr. Res.* **2023**, *338*, 1469–1476.
- (35) Miyatake, M.; Nishizono, S.; Kobayashi, T.; Sakatani, Y.; Matsubara, J.; Yamaguchi, M. Structure elucidation of the active polysaccharide component in Hyuganatsu Orange (*Citrus tamurana* Hort. ex Tanaka) and its effect on osteoclast formation. *Food Sci. Technol. Res.* **2021**, *27* (6), 907–914.
- (36) Tang, S.; Wang, T.; Huang, C. X.; Lai, C. H.; Fan, Y. M.; Yong, Q. Arabinogalactans from Larix principis-rupprechtii: An investigation into the structure-function contribution of side-chain structures. *Carbohydr. Polym.* **2020**, *227*, 115354.
- (37) Qi, H.; Tang, S.; Bian, B.; Lai, C.; Chen, Y.; Ling, Z.; Yong, Q. Effect of H₂O₂-VC degradation on structural characteristics and immunomodulatory activity of larch arabinogalactan. *Front. Bioeng. Biotechnol.* **2024**, *12*, 1461343.
- (38) Fry, S. C. Cross-linking of matrix polymers in the growing cell walls of angiosperms. *Annu. Rev. Plant Phys.* **1986**, *37*, 165–186.
- (39) Basanta, M. F.; Plá, M. F. D.; Stortz, C. A.; Rojas, A. M. Chemical and functional properties of cell wall polymers from two cherry varieties at two developmental stages. *Carbohydr. Polym.* **2013**, *92*, 830–841.
- (40) Li, Z. X.; Wu, L.; Wang, C.; Wang, Y.; He, L.; Wang, Z.; Ma, X.; Bai, F.; Feng, G.; Liu, J.; Jiang, Y.; et al. Characterization of pectin methylesterase gene family and its possible role in juice sac granulation in navel orange (*Citrus sinensis* Osbeck). *BMC Genomics* **2022b**, *23*, 185.
- (41) El-Nawawi, S. A.; Heikel, Y. A. Factors affecting gelation of high-ester citrus pectin. *Process Biochem.* **1997**, *32* (5), 381–385.
- (42) Lee, H.; Rivner, J.; Urbauer, J. L.; Garti, N.; Wicker, L. De-esterification pattern of Valencia orange pectinmethylesterases and characterization of modified pectins. *J. Sci. Food Agric.* **2008**, *88*, 2102–2110.
- (43) Sousa, A. G.; Nielsen, H. L.; Armagan, I.; Larsen, J.; Sørensen, S. O. The impact of rhamnogalacturonan-I side chain monosaccharides on the rheological properties of citrus pectin. *Food Hydrocolloids* **2015**, *47*, 130–139.
- (44) Yao, J. Q.; Yang, C.; Shi, K. X.; Liu, Y. Z.; Xu, G.; Pan, S. Y. Effect of pulp cell wall polysaccharides on citrus fruit with different mastication traits. *Food Chem.* **2023**, *429*, 136740.
- (45) Qin, Z.; Liu, H. M.; Lv, T. T.; Wang, X. D. Structure, rheological, thermal and antioxidant properties of cell wall polysaccharides from Chinese quince fruits. *Int. J. Biol. Macromol.* **2020**, *147*, 1146–1155.



CAS BIOFINDER DISCOVERY PLATFORM™

STOP DIGGING THROUGH DATA — START MAKING DISCOVERIES

CAS BioFinder helps you find the right biological insights in seconds

Start your search

